OPTOELECTRONICS AND ADVANCED MATERIALS – RAPID COMMUNICATIONS Vol. 4, No. 6, June 2010, p. 871 - 876

# Calibration method for dosimetric films

A. SCARISOREANU*, F. SCARLAT, S. BERCEA[a], R. POPA[b]
*National Institute for Laser, Plasma and Radiation Physics INFLPR, Bucharest, Romania*
[a] *"Horia Hulubei" National Institute of Physics and Nuclear Engineering – IFIN HH, Bucharest, Romania*
[b] *„Prof. Dr. Al. Trestioreanu" Oncologic Institute Bucharest, Romania*

A dosimetric film Kodak X OMATV type was investigated to obtain a calibration curve, using a fast densitometric method. Film was irradiated by a 6 MeV X-ray beam, at different doses and different radiation fields. The method is applicable for any type of medical films. Films are the most frequently used for patient treatment quality assurance, in different medical domains. Present work shows the experimental results obtained with the film densitometer from MULTIDATA System – USA, outfitted with RTD4 software, 5.2 version, for two pulmonary radiographies to evidence the areas where suspiciuous formation are located and to help the radiologist to elaborate a corect planing treatment. The method can be used for tracing and and locating other tumor in the human body as well.

(Received April 19, 2010; accepted June 16, 2010)

*Keywords*: Isodensitometric method, Absorbed dose distribution, Film densitometer

## 1. Introduction

Ionizing radiation study is very important because the ionizing radiation has a great impact upon the living matter. The ionizing radiation used in medicine for radiation diagnose and radiation therapy, is very useful because along with other practices, they aim at improving life quality of the people that are early diagnosed, with different kinds of cancer, beginning with a simple bone crack, to different cancers.

One of the advantages of using film in 1D (depth dose distribution), 2D (isodose distribution) and 3D (spatial representation of a film surface scanning) dose distribution determinations, is the fast time in obtaining them. Film can be placed in different radiation fields and it permits data acquisition on a large surface. Another advantage is the short time needed for to obtain the film, using a low radiation dose. The process to obtain radiography is an excellent practice used in the medical domain, for the relative measurement of the dose distribution. This paper presents the dose distribution obtained by the isodensitometry method for the determination of irradiation external field parameters used in radiation diagnose and radiation therapy. A similar method is used for personal dosimetry at IFIN-HH, using another type of film densitometer. The dose distributions were obtained using a film densitometer. It can be used to obtain the calibration curve (film response curve, the relation between optical density and absorbed dose) for different type of film.

Cancer is a main cause of death and worldwide, the total number of cancer cases is increasing. Some types of cancer appear rarely (e.g. stomach cancer) and others appear in a bigger number (e.g. malign melanoma – a dangerous type of skin cancer). The lung cancer [1] is more frequent at men than women in most countries particularly with the young people. In other countries the number of persons diagnosed with lung cancer is growing for both sexes. Although smoking remains the main cause of this type of cancer, it is also present with nonsmokers too, but in a limited number. For example, a study elaborated in Sweden, showed the rates of 4.8 (male) and 14.4 (female) [2] per 100,000 person-years for never smokers age 40 to 79 years were. Pulmonary medicine is strongly based on plain chest radiography. Indeed, chest radiography is the single most common investigation practice carried out in hospitals [3].

## 2. Materials and methods

The photographic films were used for first time for the detection of natural radiation [4].

After x-ray radiation discovery, the film applications in medicine became very important and consequently radiologists were trained [5], to interpret the radiographies.

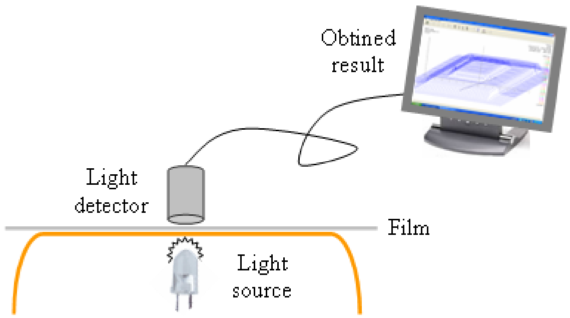


*Fig. 1. Schematic representation of an optical densitometer.*

The MULTIDATA Film Densitometer 9721type, is reading the blackening densities in ADCU values (Analog to Digital Conversion Unit), which correspond to certain doses and, employing some special dedicated software, the dosimeter gives the calibration curve corresponding to the investigated film. This paper is also presenting the results obtained, after the investigations made with the film densitometer, for two pulmonary radiographies.

The densitometer (Fig. 1) is outfitted with a collimated light source placed under a sensible light detector, which records the value of the optical densities on the film.

The RTD4 software is installed on the notebook where the film densitometer is connected to, is working with “RRP Properties” program (Fig. 2) where are introduced the ADCU values corresponding to each irradiated surface on the film and the dose values was irradiated to each film surface.

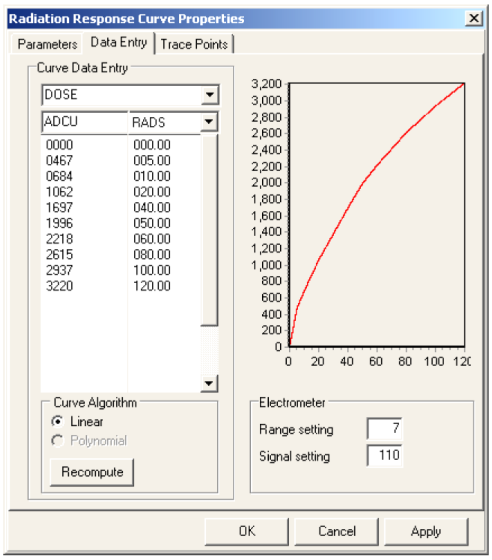


*Fig. 2. Example of radiation response curve in “RRC properties” [4].*

Next the program shows the corresponding calibration curve. The film (Fig. 3) investigated in this experiment, is a Kodak film X OMATV type, used in hospitals for X-ray and γ-ray dosimetry, using the medical linear accelerator existing in „Prof. Dr. Al. Trestioreanu” Oncologic Institute Bucharest, Romania.

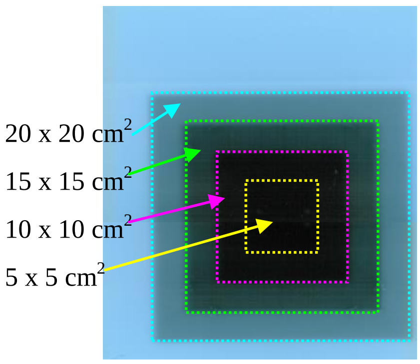


*Fig. 3. Presentation of the irradiated medical dosimetric film.*

The film was introduced in a special alignment device and placed at 100 cm distance, i. e. the reference standard distance SSD (Source to Surface Distance).

First, the film was irradiated with an X-ray beam of 10 cGy dose throughout the film irradiated surface to form a square radiation field with the surface equal with 20 x 20 $cm^2$. Next the film kept in the same position, was irradiated in turn with X-ray beams having the same dose and the same shape, each surface being smaller by 5 x 5 $cm^2$, till a surface equal with 5 x 5 $cm^2$ was reached.

Table 1 displays the radiation field size and the absorbed dose to film, used for obtaining the investigated film.

*Table 1. Radiation field dimensions and dose values used for obtaining the investigated film.*

| No. | Radiation field dimension [$cm^2$] | Radiation dose [cGy] |
|---|---|---|
| 1 | 20 x 20 | 10 |
| 2 | 15 x 15 | 20 |
| 3 | 10 x 10 | 30 |
| 4 | 5 x 5 | 40 |

The dozimetric films obtained in different locations of the human body can be investigated in several ways, e.g. the use of negatoscope. In case of the physical method used for this paper, the films were investigated using MULTIDATA Film Densitometer.

The densitometer is reading the information related to blackening densities from the film, using a detector – light source assembly. The obtained information is next represented in 2D, 3D blackening distributions, blackening isodensities respectively, which are equivalent to the dose reaching to the film. After passing through tissues with small volume density (e.g. lungs), the radiation coming to the film in a large quantity than when passing through tissues with a larger volume density (e.g. bone), because is attenuated by the respective tissue.

The literature [6] is specifies that in particular, the mammary glands which show a big collagen density, are liable to occur of cancer tumors and to metastasis consequently. On the mammography the surfaces in which the tumors are located, have a smaller blackening density then in the places of healthy mammary tissue, because the volume density of the tumor is bigger than the density of the surrounding healthy tissue and a big part of the dose is attenuated by the tumor.

From 2D, 3D blackening distribution and blackening isodensities corresponding to radiographic film, tumor localisation and dimensions can be traced and interpreted.

## 3. Results and discussion

### 3.1 The medical dosimetric film investigation

The film blackening (answer) is evaluated in ADCU values, which can be quantitatively determined using a densitometer.

Fig. 4 presents a 2D blackening distribution of the dosimetric film presented in Fig. 3, in which 49 curves resulted after the scanning of the dosimetric film surface can be seen.

The reading points for ADCU values where choosen at 0.5 cm distance, so to contain all film surfaces with different blackening densities. The highest “step” in Fig. 4 is given by the film surface with 5 × 5 $cm^2$ area, which showed the biggest blackening density, given by a successive accumulated dose equal with 40 cGy.

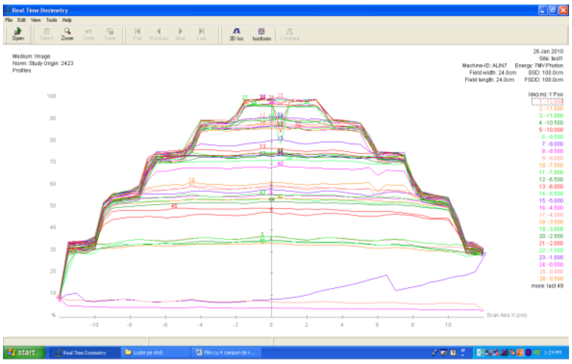

*Fig. 4. 2D blackening distribution corresponding to medical dosimetric film in Fig. 1.*

Fig. 5 shows the 3D blackening densities distribution on the dosimetric film.

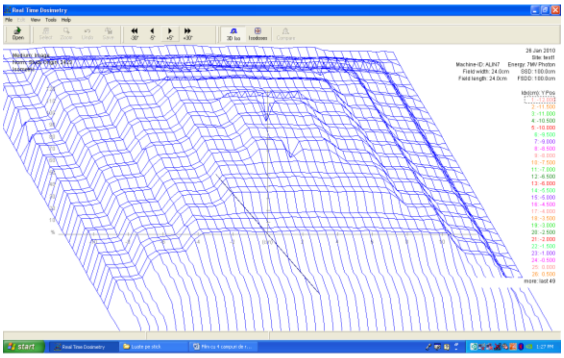

*Fig 5. 3D blackening distribution for the film in Fig. 1.*

The next 3 “steps” are given by the others three surfaces on the film, with blackening densities smaller and smaller and the last “step” is given by the film surface which wasn’t exposed to radiations.

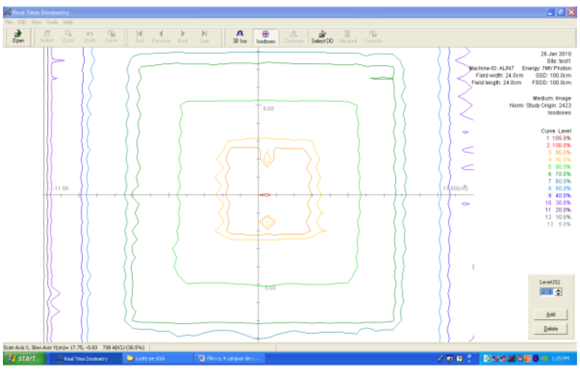

*Fig. 6. Blackening isodensity distributions recorded by the medical dosimetric film in Fig. 1.*

Fig. 6 presents the blackening isodensitiy distributions which are equivalent with the isodose distributions recorded on the film. It can be seen here that the uniformity of the radiation field is having different dimensions. The surface in the center of the figure, surrounded by the orange line, represents the surface on the film on which 40 cGy was applied. In this area there are also evidences of the marks made by the medical physicist on the film to make a better radiation field alignment for the radiation fields that were used.

For choosing the ADCU values used to calibration curve representation corresponding to the dosimetric film in Fig. 3, one scanning curve passing over the center of all the 4 surfaces with different blackening densities and numbered curve 23 was selected (Fig. 7).

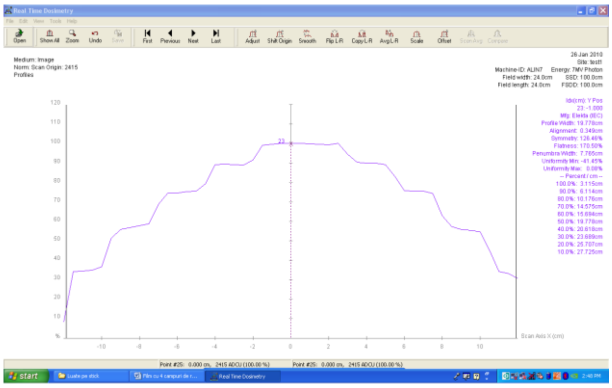

*Fig 7. The curve number 23 from which the ADCU values used to obtain the calibration curve specific to the film in Fig. 1 were determined.*

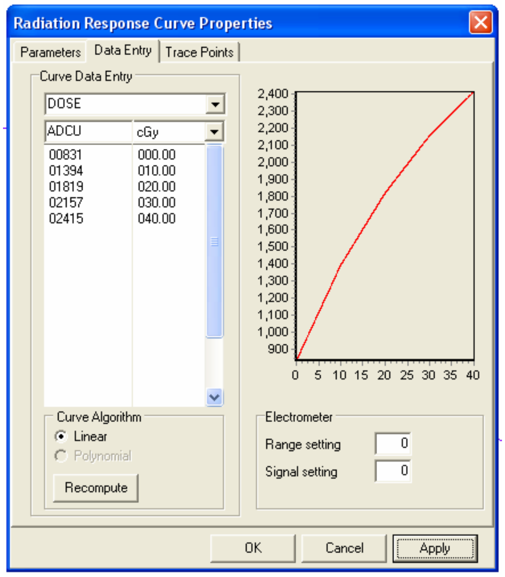


*Fig. 8. The program used to obtain the calibration curve specific to investigated film.*

As specified above, the RTD4 software was employed with “RRC properties” (Fig 8) where the ADCU values corresponding to all the 4 irradiated surfaces on the film, to the non-irradiated surface and the dose radiation values reached on each surface were entered.

Next the program drawn the corresponding calibration curve. Fig. 9 shows the calibration curve in a larger range, on which the dose values corresponding to any ADCU value, including in the investigated range can be determined, by simply placing the mouse cursor on the curve. For example (Fig. 8) in the point where the yellow star is placed, for ADCU = 1500, the dose is equal to 12.5 cGy.

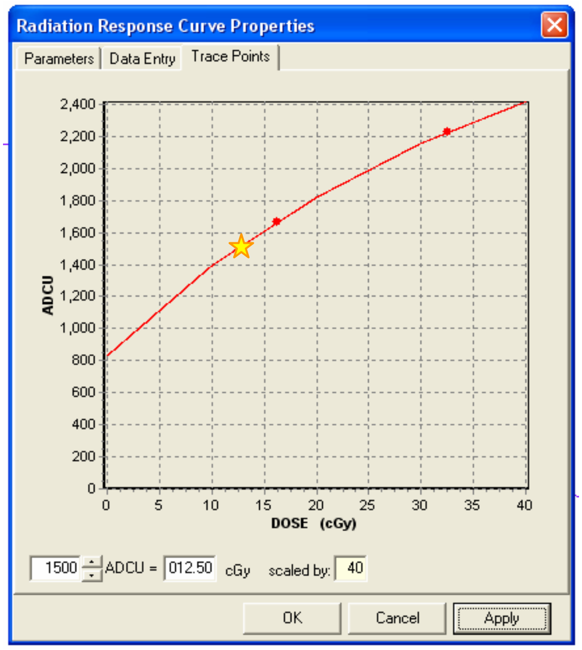


*Fig. 9. The calibration curve corresponding to the film in Fig. 3.*

Table 2 includes the dose values accumulated on the dosimetric film, dependent on the blackening densities expressed in ADCU values.

*Table 2. The dose values corresponding to the doses recorded on the dosimetric film.*

| Dose (cGy) | Blackening density (ADCU) |
|---|---|
| 0,0 | 0 |
| 10,0 | 1396,8 |
| 12,5 | 1500 |
| 15,0 | 1606 |
| 17,5 | 1713 |
| 20,0 | 1819 |
| 22,5 | 1903,3 |
| 25,0 | 1988,2 |
| 27,5 | 2065,6 |
| 30,0 | 2156,5 |
| 32,5 | 2221,5 |
| 35,0 | 2285,2 |
| 37,5 | 2350,3 |
| 40,0 | 2415 |

The dose values between that presented in Table 2, can be found by interpolation.

### 3.2 Lung radiography investigation

The lung radiography is an important medical procedure, being the common and faster procedure one used in lung investigations.

Fig. 10 presents the radiography of the thoracic zone, where different trauma areas in the case of accidents may occur: 1. – fracture of the ribs 1 – 3; 2. loss of lung pleural edge; 3. fractured ribs at curve apices; 4. widening of superior mediastinum indicates vessel rupture; 5. fluid such as blood is present;

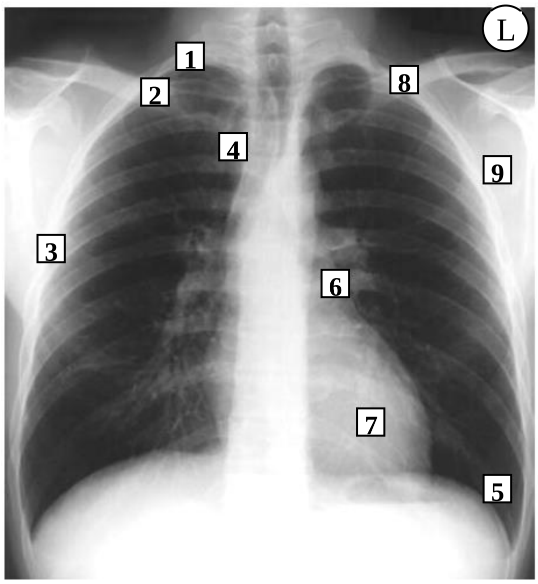


*Fig. 10. Radiography of a human and the places where different trauma in the thoracic zone can be seen [5].*

6. air infiltration in the tissue existing in the space between lungs; 7. liquid accumulation in pericardium („bag” in which is the heart); 8. fracture of the clavicle; 9. fracture of shoulder ligament.

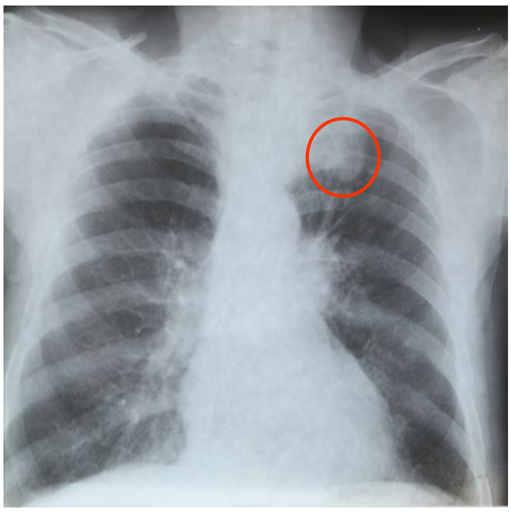

*Fig. 11. Pulmonary radiography which presents a suspect formation, in the clavicle area in the left part.*

Further a pulmonary radiography (Fig. 11), presenting a suspect formation was investigated, using the film densitometer. It can be seen that the pulmonary radiography presents a heterogeneous opacity, of approximate 2 cm diameter under clavicle in the left part, where the blackening density is low. There is the suspicion that, in that area, a tumoral formation is present. Fig. 12 presents the 2D blackening distribution corresponding to the investigated pulmonary radiography, in Fig. 11.

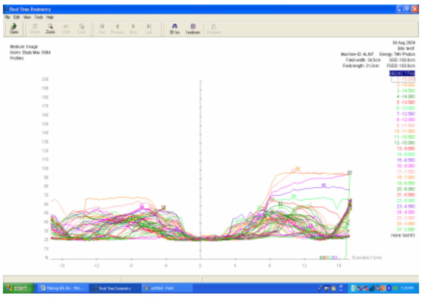

*Fig. 12. 2D blackening distribution corresponding to the pulmonary radiography in Fig. 11.*

Blackening distributions between 70 % and 100 %, corresponding to the film area where the blackening density is the biggest are shown. The dose reaching at that film area was high because it came directly to the film and the radiations were not attenuated by any tissue. The central area of the 2D blackening distribution, with the smallest blackening percentage is corresponding to the surface where the stern and spine are present, and where the biggest part of the radiation dose was absorbed by them, and to the film were only a little part of it has reached.

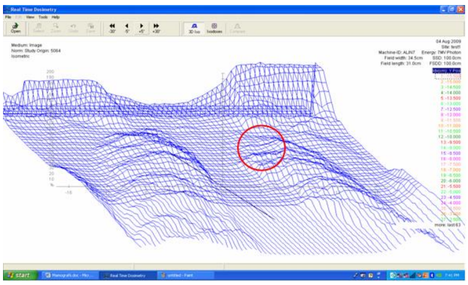

*Fig. 13. 3D blackening distribution corresponding to pulmonary radiography in Fig. 11; view from abdomen to cervical area.*

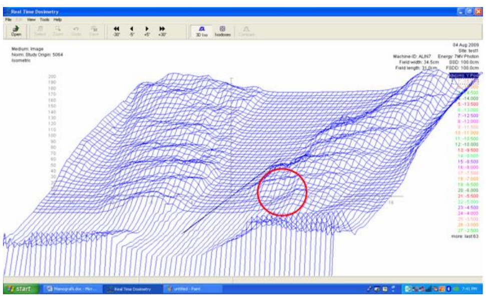

*Fig. 14. 3D blackening distribution corresponding to pulmonary radiography in Fig. 11; view from cervical area to abdomen.*

The rest of the blackening distributions are given by that area in which the lungs are placed, together with the area in the left under the clavicle in which the existence of a tumoral formation is assumed.

Fig. 13 and Fig. 14 present the 3D blackening distributions of the pulmonary radiography in Fig. 11, with views from two different angles. In both figures by a red circle, the under clavicle tumoral formation is marked. Fig. 15 shows the blackening isodensities distribution corresponding to the pulmonary radiography presented in Fig. 11, where the left under clavicle tumoral formation is marked by a red circle too.

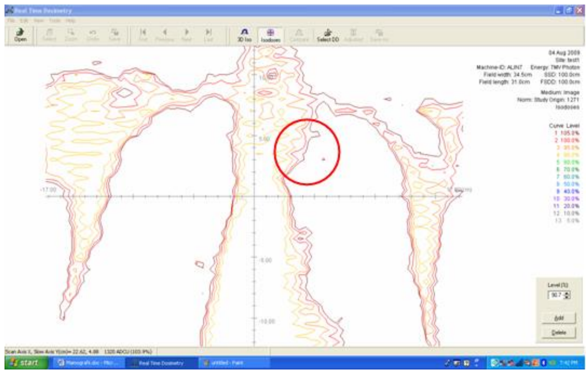

*Fig. 15. Blackening isodose distributions corresponding to pulmonary radiography in Fig 11.*

Next, the results obtained after the investigation using the Film Densitometer, of a pulmonary radiography are presented (Fig. 16) and show two fibrous calcifications under clavicles, which represent the continuation of an old tuberculosis disease.

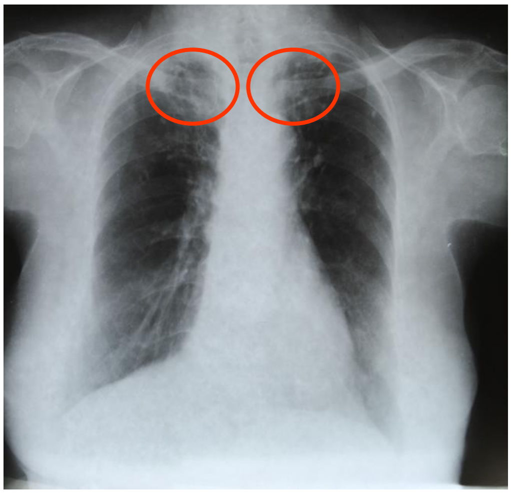

*Fig. 16. Pulmonary radiography showing 2 bi-lateral fibrous calcifications, above and under clavicle.*

Both fibrous calcifications, supposed to be tumoral formations, are presented on the radiography like two areas with smaller blackening densities then the areas where the lungs are placed.

Fig. 17, presents the 2D blackening distributions corresponding to the pulmonary radiography in Fig. 16, where one can seen three areas with three main blackening densities, as follows: the blackening distributions between 60 % and 100 % are given by the film areas on which the radiation reached directly, without being attenuated by tissues; the blackening distributions between 10 % and 20 % are given by area where the stern and the spine are present, bone tissue where the radiation was absorbed in a big part, followed by a low blackening of the film; the blackening distributions between 20 % and 60 % are given by the areas where the lungs are placed.

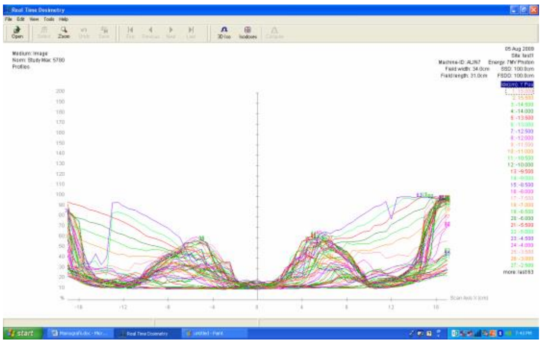

*Fig. 17. 2D blackening distribution corresponding to pulmonary radiography in Fig. 16.*

Fig. 18 shows the 3D blackening distribution corresponding to the pulmonary radiography in Fig. 16.

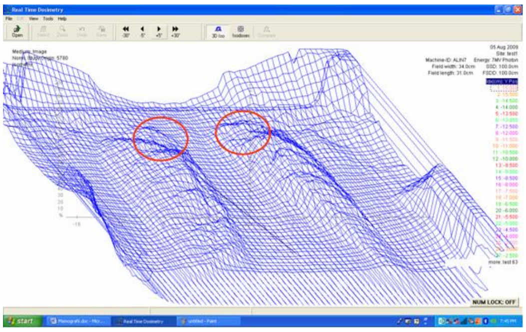

*Fig. 18. 3D blackening distributioncoresponding to pulmonary radiography in Fig. 16.*

In the clavicle area one can see observed two surfaces where the blackening distributions have low values, since these are the areas where the suspect tumoral formation is located. These areas are marked by red circles.

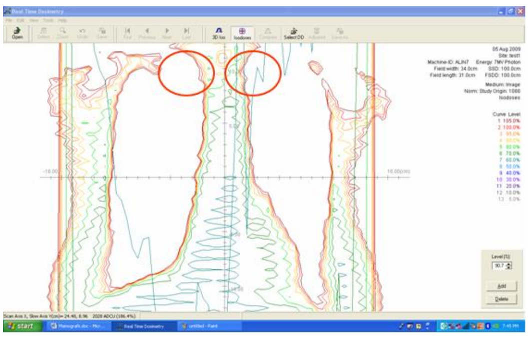

*Fig. 19. Blackening isodensities distributions corresponding to the pulmonary radiography in Fig. 16.*

Blackening isodose distributions from the pulmonary radiography in Fig. 16 are presented in Fig. 19.

A red circle surrounds the area where the fibrous calcifications are present and which have a lower blackening density than the rest of the areas where the lungs are placed.

## 4. Conclusions

The method presented in the first experimental part of this work, evidences the dose distribution uniformity for all areas in the dosimetric field used. For the same film the corresponding calibration curve was obtained and it is very useful to check the stability in time of the radiation beam. It is very important that the radiation beam, before being used in radiation diagnose or radiation therapy, should be carefully investigated namely to determine the beam distribution uniformity.

The results obtained after two pulmonary radiography investigations leads to point out the suspect areas, helping thus the radiologist to make a more correct treatment planning, and the used method can be applicable to locate any tumor in the human body as well.

Dose distribution uniformity on the film is very important because it permits the identification of formations with different attenuation.

## References

[1] J. Ferlay, O. Autier, M. Boniol, M. Heanue, M. Colombet, P. Boyle, Ann. Oncol. **18**(3), 2007.

[2] H. A. Wakelee, E. T. Chang, L. S. Gomez, H. T. Keegan, D. Feskanich, A. C. Clarke, L. Holmberg, C. L. Yong, N. L. Kolonel, K. M. Gould, W. D. West, Journal of Clinical Oncology **25**(5), 2007.

[3] P. Eng, F. - K. Cheah, Interpreting chest X-rays illustrated with 100 cases, Cambridge University Press, 2005.

[4] A. Scarisoreanu, F. Scarlat, R. Popa, Opt. Adv. Mater. – Rapid Comm. **3**(12), 1321 (2009).

[5] J. McConnell, R. Eyres, J. Nightingale, Interpreting Trauma Radiographs, Blackwell Publishing Ltd, 2005.

[6] S. Vedantham, A. Karellas, S. Suryanarayanan, D. Albagli, S. Han, E. J. Tkaczyk, C. E. Landberg, B. Opsahl-Ong, P. R. Granfors, I. Levis, C. J. D'Orsi, R. E. Hendrick, Med. Phys. **27**, 2000.

*Corresponding author: a_m_mihalache@yahoo.com